arXiv:1201.2608v2 [hep-ph] 20 Mar 2012

Leading logarithms in the anomalous sector of two-flavour QCD

Johan Bijnens[a], **Karol Kampf**[b,a] **and Stefan Lanz**[a]

[a] Department of Astronomy and Theoretical Physics, Lund University
Sölvegatan 14A, S 223 62 Lund, Sweden

[b] Institute of Particle and Nuclear Physics,
Faculty of Mathematics and Physics,
Charles University, 18000 Prague, Czech Republic.

Abstract

We add the Wess-Zumino-Witten term to the $N = 3$ massive nonlinear sigma model and study the leading logarithms in the anomalous sector. We obtain the leading logarithms to six loops for $\pi^0 \to \gamma^* \gamma^*$ and to five loops for $\gamma^* \pi \pi$. In addition we extend the earlier work on the mass and decay constant to six loops and the vector form factor to five loops. We present numerical result for the anomalous processes and the vector form factor. In all cases the series are found to converge rapidly.

Keywords: Renormalization group evolution of parameters; Spontaneous and radiative symmetry breaking; Chiral Lagrangians; Anomalous processes

Contents

1   Introduction

Obtaining exact results in quantum field theory is rather difficult. One of the few things which can be easily calculated to all orders in renormalizable theories are the leading logarithms of the type $(g^2 \log \mu^2)^n$ where μ is the subtraction scale and g the coupling constant. The analogue of this in effective field theories is not so simple since at each order in the expansion new terms in the Lagrangian appear and the recursive argument embedded in the renormalization group equations for renormalizable theories no longer applies. Nonetheless, one can calculate the leading logarithms in effective field theories using only one-loop calculations. This was suggested at two-loop order by Weinberg [1] and proven to all orders in [2].

In the massless case this has been used to very high orders in [3–5] for meson-meson scattering and form factors. In the massive case, many more terms contribute but in [6, 7] a method was developed for handling those, and the leading logarithms in the massive nonlinear sigma model were obtained to five-loop order for the mass, decay constant and the vacuum expectation value and to four-loop order for the vector and scalar form factors and the meson-meson scattering amplitude. A natural continuation of that program is to extend it to other sectors as well. We therefore add to the massive nonlinear sigma

1

model for $N = 3$ the anomalous part via the Wess-Zumino-Witten (WZW) term. This allows us to study the leading logarithms for anomalous processes in two-flavour Chiral Perturbation Theory (ChPT). In addition one can hope that in this sector with its many nonrenormalization theorems it might be easier to guess the all order results when the first terms in the series are known. The WZW term only makes sense for $N = 3$ so we do not work out the results for general N in this case.

We have also improved the programs used in [6, 7] so that they now can be used to arbitrarily high orders given enough computing power. So, at least in principle, the problem of the leading logarithms is solved. In practice we obtained one order more than in the earlier work.

The main part of the paper is devoted to the calculations of the leading logarithms (LL) for the two main anomalous processes in the pion sector, the full $\pi^0\gamma^*\gamma^*$ and $\gamma^*\pi\pi\pi$ vertices. For the former we obtained the LL to six loops and for the latter to five. The results indicate that in all cases the chiral expansion converges fast but we did not find a simple all-order conjecture.

The results agree with all known relevant earlier calculations. As an additional check we have used several different parametrizations of the fields.

In Sect. 2.1 we introduce shortly the massive nonlinear sigma model and in Sect. 2.2 the two-flavour Wess-Zumino-Witten term. Sect. 3 contains the discussion of LL in the nonanomalous sector where we present our new results and show some numerical results. Here we also explain briefly the principles of the calculation. More details on the method can be found in [6, 7]. Sects. 4 and 5 are the main part of this paper. The LL are calculated in Sect. 4. We did not find a simple all-order conjecture but the LL indicate for example that the nonfactorizable part in $\pi^0\gamma^*\gamma^*$ with both photons off shell should be small. We present numerical results in Sect. 5. In all cases we find good convergence. Sect. 6 shortly recapitulates our results. The appendix contains a dispersive argument to clarify the discrepancy with [4] for the vector form factor.

2 The model

2.1 Massive nonlinear $O(N+1)/O(N)$ sigma model

The $O(N+1)/O(N)$ nonlinear sigma model, including external sources, is given by the Lagrangian

$$\mathcal{L}_{n\sigma} = \frac{F^2}{2} D_\mu \Phi^T D^\mu \Phi + F^2 \chi^T \Phi \,. \tag{1}$$

Φ is a real $N+1$ vector, $\Phi^T = \begin{pmatrix} \Phi^0 & \Phi^1 & \dots & \Phi^N \end{pmatrix}$, which satisfies the constraint $\Phi^T \Phi = 1$ and transforms under the fundamental representation of $O(N+1)$. The covariant derivative is

$$\begin{aligned} D_\mu \Phi^0 &= \partial_\mu \Phi^0 + a^a_\mu \Phi^a \,, \\ D_\mu \Phi^a &= \partial_\mu \Phi^a + v^{ab}_\mu \Phi^b - a^a_\mu \Phi^0 \,. \end{aligned} \tag{2}$$

2

The vector sources are antisymmetric, $v_\mu^{ab} = -v_\mu^{ba}$, and correspond to the unbroken group generators. The axial sources a_μ^a correspond to the broken generators. Lower-case Latin indices $a, b, \ldots$ run over $1, \ldots, N$ in the remainder and are referred to as flavour indices. The mass term $\chi^T \Phi$ contains the scalar, s^0, and pseudoscalar, p^a, external sources as well as the explicit symmetry breaking term M^2:

$$\chi^T = \left(\; (2Bs^0 + M^2) \;\; p^1 \;\; \ldots \;\; p^N \right) . \tag{3}$$

The vacuum condensate

$$\langle \Phi^T \rangle = (1 \; 0 \; \ldots \; 0) \tag{4}$$

breaks $O(N+1)$ spontaneously to $O(N)$. We thus have in principle N Goldstone bosons represented by ϕ. The explicit symmetry breaking term, the part containing M^2, breaks the $O(N+1)$ symmetry to $O(N)$, enforcing the vacuum condensate to be in the direction (4) and gives a mass to the Goldstone bosons which at tree level is exactly M.

This particular model is the same as lowest-order two-flavour ChPT for $N = 3$ [8, 9] and has been used as a model for strongly interacting Higgs sectors in several scenarios; see, e.g., [10, 11].

The terminology for the external sources or fields is taken from two-flavour ChPT. The vector currents for $N = 3$ are given by $v^{ab} = -\varepsilon^{abc} v^c$ with ε^{abc} the Levi-Civita tensor. The electromagnetic current at lowest order is associated with v^3.

We write Φ in terms of a real N-component vector ϕ, which transforms linearly under the unbroken part of the symmetry group $O(N)$. We have made use of five different parametrizations in order to check the validity of our results. They are

$$\Phi_1 = \begin{pmatrix} \sqrt{1 - \frac{\phi^T \phi}{F^2}} \\ \frac{\phi}{F} \end{pmatrix} , \qquad \Phi_2 = \frac{1}{\sqrt{1 + \frac{\phi^T \phi}{F^2}}} \begin{pmatrix} 1 \\ \frac{\phi}{F} \end{pmatrix} ,$$

$$\Phi_3 = \begin{pmatrix} 1 - \frac{1}{2} \frac{\phi^T \phi}{F^2} \\ \sqrt{1 - \frac{1}{4} \frac{\phi^T \phi}{F^2}} \frac{\phi}{F} \end{pmatrix} , \qquad \Phi_4 = \begin{pmatrix} \cos \sqrt{\frac{\phi^T \phi}{F^2}} \\ \sin \sqrt{\frac{\phi^T \phi}{F^2}} \frac{\phi}{\sqrt{\phi^T \phi}} \end{pmatrix} ,$$

$$\Phi_5 = \frac{1}{1 + \frac{\phi^T \phi}{4F^2}} \begin{pmatrix} 1 - \frac{\phi^T \phi}{4F^2} \\ \frac{\phi}{F} \end{pmatrix} . \tag{5}$$

Φ_1 is the parametrization used in [8], Φ_2 a simple variation. Φ_3 is such that the explicit symmetry breaking term in (1) only gives a mass term to the ϕ field but no vertices. Φ_4 is the parametrization one ends up with if using the general prescription of [12]. Finally, Φ_5 has been used by Weinberg in, e.g., [1, 9]. The reason for using different parametrizations is that for each one of them, the contributions are distributed very differently between the diagrams and obtaining the same result thus provides a thorough check on our calculations.

3

2.2 Wess-Zumino-Witten Lagrangian

For $N = 3$, the massive nonlinear $O(N+1)/O(N)$ sigma model corresponds to two-flavour chiral perturbation theory, which is an effective field theory for QCD. It is well known that the chiral axial current of the latter is anomalous [13–16], leading to the occurrence of processes such as $\pi^0 \to \gamma\gamma$ or $\pi\gamma \to \pi\pi$. The Lagrangian that we have introduced above does, however, not account for this. The necessary interaction terms are contained in the Wess-Zumino-Witten term [17, 18], which must be added to the effective Lagrangian. It is constructed such that it reproduces the anomalous Ward identities. Kaiser derived the WZW term for two-flavour ChPT [19], where it is considerably simpler than in the case of three flavours. His result can be re-expressed in terms of the field Φ as

$$\mathcal{L}_{WZW} = -\frac{N_c}{8\pi^2}\epsilon^{\mu\nu\rho\sigma}\left\{\epsilon^{abc}\left(\frac{1}{3}\Phi^0\partial_\mu\Phi^a\partial_\nu\Phi^b\partial_\rho\Phi^c - \partial_\mu\Phi^0\partial_\nu\Phi^a\partial_\rho\Phi^b\Phi^c\right)v_\sigma^0\right.$$
$$\left. + (\partial_\mu\Phi^0\Phi^a - \Phi^0\partial_\mu\Phi^a)v_\nu^a\partial_\rho v_\sigma^0 + \frac{1}{2}\epsilon^{abc}\Phi^0\Phi^a v_\mu^b v_\nu^c \partial_\rho v_\sigma^0\right\}. \tag{6}$$

The interaction with the axial current coming from the WZW term has been omitted. Note that the normalization of the vector field differs from the one used in [19]. The Lagrangian depends on the Levi-Civita tensor ϵ^{abc} in the $SO(3)$ flavour indices. This is an object specific to $N = 3$. There is no obvious simple generalization[1] to different N so for anomalous processes we restrict the calculation to $N = 3$.

The Lagrangian in (6) is of chiral order p^4 implying that anomalous processes are of the same order at leading order, while one-loop corrections are already $\mathcal{O}(p^6)$. This is immediately clear from the presence of the epsilon tensor with four Lorentz indices: each one of them must be combined with either a derivative or an external vector field, both of which are $\mathcal{O}(p)$.

The interaction of the pseudoscalars with the photon field $\mathcal{A}_\mu$ can be obtained from the WZW Lagrangian by setting the vector current to

$$v_\mu^0 = \frac{e}{3}\mathcal{A}_\mu, \qquad v_\mu^a = e\mathcal{A}_\mu\delta^{a3}. \tag{7}$$

The Lagrangian of (1) has also a symmetry that QCD does not have [18]. The fields under this extra symmetry, called intrinsic parity, transform as

$$\Phi^0 \to \Phi^0, \quad \Phi^a \to -\Phi^a, \quad v_\mu^{ab} \to v_\mu^{ab}, \quad a_\mu^a \to -a_\mu^a, \quad s \to s, \quad p \to -p. \tag{8}$$

The Lagrangian (1) and higher orders are even under this symmetry while (6) is odd.

As in the even sector, we have used several of the parametrizations given in (5). Intrinsic parity for the different ϕ is such that it is always odd, $\phi^a \to -\phi^a$. The WZW term leads to interactions of one, two, or three photons with an odd number of pions. The anomaly also generates purely mesonic interactions among an odd number of five or more Goldstone

---

[1]The generalization to different n for the $SU(n) \times SU(n)/SU(n)$ case is easy but that is a different case than the $O(N+1)/O(N)$ considered here.

bosons. However, for two flavours the purely mesonic odd intrinsic parity processes vanish to all orders.

We use anomalous and odd intrinsic parity as synonyms and refer to the $N = 3$ case here occasionally as the two-flavour case since it corresponds to two light quark flavours.

3   Leading logarithms in the even sector

In this section we recapitulate and extend some results of the even intrinsic parity sector of [6, 7]. We focus on those results that will be needed for the later calculations in the anomalous sector.

The leading dependence on $\log \mu$ at each order, with μ the subtraction scale, is what we call the leading logarithm. It can in principle always be obtained from one-loop calculations as was proven using β-functions in [2] and in a simpler diagrammatic way in [6]. We will discuss some of those results in the sections on the explicit calculation of the mass and $\gamma \pi \to \pi \pi$.

In effective field theories there is a new Lagrangian at every order. The observation of [6] that the needed parts of those Lagrangians can be generated automatically from the one-loop diagrams allowed to perform the calculations. The actual calculations were performed by using FORM [20] extensively.

We have extended the programs used in [6, 7] so that they can in principle run to an arbitrary order[2]. The only limit is set by computing time, which grows rapidly with the order. The necessary additions include routines that generate the required diagrams at a given order and calculate one-loop diagrams with an arbitrary number of propagators. In this way, we have verified some of the earlier results and obtained the coefficient of one more order for the mass, decay constant and vector form factor.

In effective field theories writing the expansion in terms of lowest order or physical quantities can make quite a big difference in the rate of convergence. We therefore follow [7] in using two different expansions in terms of leading logarithms. A given observable O_{phys} can be written in different ways:

$$O_{\text{phys}} = O_0 \left(1 + a_1 L + a_2 L^2 + \cdots \right) , \tag{9}$$
$$O_{\text{phys}} = O_0 \left(1 + c_1 L_{\text{phys}} + c_2 L_{\text{phys}}^2 + \cdots \right) , \tag{10}$$

where the chiral logarithms are defined either from the lowest-order parameters M and F as

$$L \equiv \frac{M^2}{16\pi^2 F^2} \log \frac{\mu^2}{M^2} , \tag{11}$$

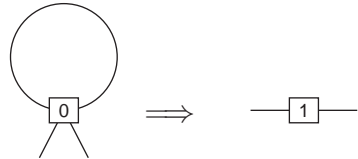or from the physical decay constant F_π and mass M_π as

$$L_{\text{phys}} \equiv \frac{M_\pi^2}{16\pi^2 F_\pi^2} \log \frac{\mu^2}{M_\pi^2} . \tag{12}$$

---

[2]In [6, 7], a different program was used for each diagram with a given number of vertices/propagators and the list of possible diagrams was constructed by hand.
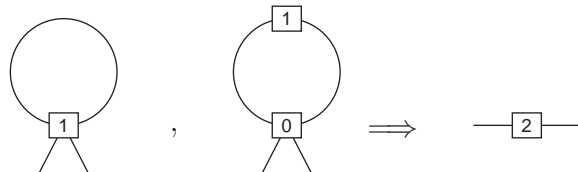
3.1 Mass

In this subsection we will present the first few coefficients a_i and c_i of the expansions in (9) and (10) with $O_{\text{phys}} = M_\pi^2$ and $O_0 = M^2$. In addition, we have also calculated the generic two-point function, which is needed for the wave-function renormalization. We extend the result from [6] by giving the expansion coefficients a_i and c_i also at sixth order.

Let us briefly recapitulate the strategy that is followed to obtain the expansion coefficients. The starting point is the Lagrangian (1) which generates vertices with an arbitrary even number of pion legs. These lowest-order vertices are diagrammatically denoted by $\boxed{0}$ with the corresponding number of legs appended. The zero in this symbol refers to the order in the expansion. If we want to calculate the leading logarithm for the two-point function at one-loop level, we must evaluate the tadpole diagram with one insertion of the leading-order four-pion vertex. Its divergence must be canceled by a counter term from the next order. This can be depicted schematically as
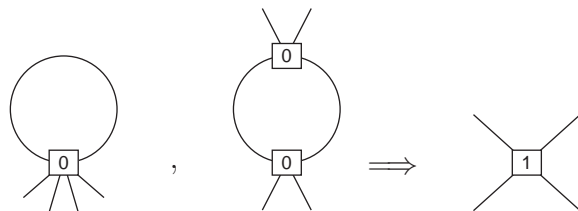
$$\qquad\qquad (13)$$

Also at the next order, divergences must cancel, but the situation is somewhat more complicated. There are two one-loop diagrams from which, using the results of [2, 6], the leading divergence can be determined. This thus determines the relevant part of the second-order Lagrangian:

$$\qquad\qquad (14)$$

We already have all information ready in order to calculate the second diagram: the tree-level vertex follows directly from the lowest-order Lagrangian and the next-to-leading-order vertex has been determined in (13). The first diagram, however, contains the next-to-leading-order vertex with four pion legs, which we do not know yet. In order to obtain its divergence, we must calculate two more diagrams:

$$\qquad\qquad (15)$$

The algorithm continues to higher orders in exactly the same way. All the diagrams needed for the two-point function up to third order are shown in [6], Figs. 3–5. The total number of diagrams needed for the mass up to order n is $1, 5, 16, 45, 116, 303, \ldots$.

i	a_i for $N = 3$	a_i for general N
1	$-1/2$	$1 - 1/2\,N$
2	$17/8$	$7/4 - 7/4\,N + 5/8\,N^2$
3	$-103/24$	$37/12 - 113/24\,N + 15/4\,N^2 - N^3$
4	$24367/1152$	$839/144 - 1601/144\,N + 695/48\,N^2 - 135/16\,N^3 + 231/128\,N^4$
5	$-8821/144$	$33661/2400 - 1151407/43200\,N + 197587/4320\,N^2 - 12709/300\,N^3$ $+6271/320\,N^4 - 7/2\,N^5$
6	$\frac{1922964667}{6220800}$	$158393809/3888000 - 182792131/2592000\,N + 1046805817/7776000\,N^2$ $-17241967/103680\,N^3 + 70046633/576000\,N^4 - 23775/512\,N^5$ $+7293/1024\,N^6$

Table 1: The coefficients a_i of the leading logarithm L^i up to $i = 6$ for the physical meson mass.

i	c_i for $N = 3$	c_i for general N
1	$-1/2$	$1 - 1/2\,N$
2	$7/8$	$-1/4 + 3/4\,N - 1/8\,N^2$
3	$211/48$	$-5/12 + 7/24\,N + 5/8\,N^2 - 1/16\,N^3$
4	$21547/1152$	$347/144 - 587/144\,N + 47/24\,N^2 + 25/48\,N^3 - 5/128\,N^4$
5	$179341/2304$	$-6073/1800 + 32351/2400\,N - 59933/4320\,N^2 + 224279/43200\,N^3$ $+761/1920\,N^4 - 7/256\,N^5$
6	$\frac{2086024177}{6220800}$	$-17467151/3888000 - 10487351/2592000\,N + 68244763/1944000\,N^2$ $-5630053/172800\,N^3 + 18673489/1728000\,N^4 + 583/2560\,N^5$ $-21/1024\,N^6$

Table 2: The coefficients c_i of the leading logarithm L^i_{phys} up to $i = 6$ for the physical meson mass.

We did not find a simple formula to estimate the total number of diagrams needed. We did find a conjecture, verified up to 12th order, about the number of diagrams needed with only two external legs at each order:

$$\#\text{ two-point diagrams} = \begin{cases} 2^{n-2} + 3 \times 2^{\frac{n-3}{2}} - 1 & \text{for } n \text{ odd} \\ 2^{n-2} + 2^{\frac{n}{2}} - 1, & \text{for } n \text{ even} \end{cases}, \quad (16)$$

that is: 1, 2, 4, 7, 13, 23, 43, 79, 151, ... diagrams with two external legs at order n.

The coefficients a_i and c_i in the expansion of the physical mass are listed up to sixth order in Tables 1 and 2. The sixth-order results are new. We can use these results to check the expansions and how fast they converge. We chose $F = 0.090$ GeV, $F_\pi = 0.0922$ GeV and $\mu = 0.77$ GeV for the plots presented here in Fig. 1.
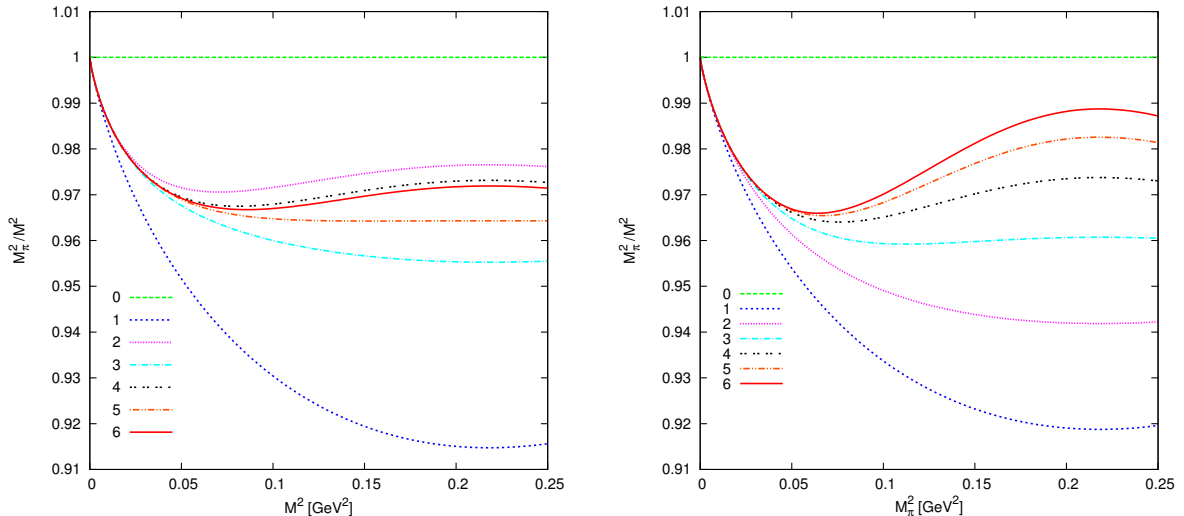
Figure 1: The contribution of the leading logarithms to M_π^2/M^2 order by order for $F = 0.090$ GeV, $F_\pi = 0.0922$ GeV, $\mu = 0.77$ GeV and $N = 3$. The left panel shows the expansion in L keeping F fixed, the right panel the expansion in L_{phys} keeping F_π fixed.

3.2 Decay constant

The decay constant F_π is defined by

$$\langle 0|j_{a,\mu}^b|\phi^c(p)\rangle = iF_\pi p_\mu \delta^{bc} . \tag{17}$$

We thus need to evaluate a matrix-element with one external axial field and one incoming meson. The diagrams needed for the wave function renormalization were already evaluated in the calculation for the mass in the previous subsection. What remains is thus the evaluation of all relevant one-particle-irreducible (1PI) diagrams with an external a_μ^a. At one-loop order there is only a single diagram, but at higher orders, we must calculate 2, 4, 7, 13, 23, ... diagrams, not counting the auxiliary diagrams required for the renormalization of higher-order vertices with more than two legs. We do not show these diagrams here, but they can be found up to third order in [7]. The total number of diagrams with an axial current that needs to be calculated for the decay constant to order n is $1, 5, 18, 56, 169, 511, \ldots$

We give the coefficients for both leading logarithm series with $O_{\text{phys}} = F_\pi$ and $O_0 = F$ in Tables 3 and 4. The sixth order is again a new result. Note that once the expression of F_π as a function of F is known one may express the remaining observables as a function of the physical M_π^2 and F_π. This has already been used to calculate the coefficients c_i in Tables 2 and 4 from the corresponding a_i.

We have plotted in Fig. 2 the expansion in terms of the unrenormalized quantities and in terms of the physical quantities. In both cases we get a good convergence but it is excellent for the expansion in physical quantities.

8

i	a_i for $N = 3$	a_i for general N
1	1	$-1/2 + 1/2\,N$
2	$-5/4$	$-1/2 + 7/8\,N - 3/8\,N^2$
3	$83/24$	$-7/24 + 21/16\,N - 73/48\,N^2 + 1/2\,N^3$
4	$-3013/288$	$47/576 + 1345/864\,N - 14077/3456\,N^2 + 625/192\,N^3 - 105/128\,N^4$
5	$2060147/51840$	$-23087/64800 + 459413/172800\,N - 189875/20736\,N^2$ $+546941/43200\,N^3 - 1169/160\,N^4 + 3/2\,N^5$
6	$-\frac{69228787}{466560}$	$-277079063/93312000 + 1680071029/186624000\,N$ $-686641633/31104000\,N^2 + 813791909/20736000\,N^3$ $-128643359/3456000\,N^4 + 260399/15360\,N^5 - 3003/1024\,N^6$

Table 3: The coefficients a_i of the leading logarithm L^i for the decay constant F_π in the case $N = 3$ and in the generic N case.

i	c_i for $N = 3$	c_i for general N
1	1	$-1/2 + 1/2\,N$
2	$5/4$	$1/2 - 7/8\,N + 3/8\,N^2$
3	$13/12$	$-1/24 + 13/16\,N - 13/12\,N^2 + 5/16\,N^3$
4	$-577/288$	$-913/576 + 2155/864\,N - 361/3456\,N^2 - 69/64\,N^3 + 35/128\,N^4$
5	$-14137/810$	$535901/129600 - 2279287/172800\,N + 273721/20736\,N^2$ $-11559/3200\,N^3 - 997/1280\,N^4 + 63/256\,N^5$
6	$-\frac{37737751}{466560}$	$-112614143/93312000 + 3994826029/186624000\,N$ $-1520726023/31104000\,N^2 + 276971363/6912000\,N^3$ $-39882839/3456000\,N^4 - 979/15360\,N^5 + 231/1024\,N^6$

Table 4: The coefficients c_i of the leading logarithm L^i_{phys} for the decay constant F_π in the case $N = 3$ and in the generic N case.

3.3 Vector form factor

Before we proceed to the discussion of anomalous processes, we turn to the last ingredient from the even intrinsic parity sector which will be used later: the vertex involving a single photon and an even number of pions. It is directly connected to the vector form factor, which is defined by

$$\langle \phi^a(p_f) | j^{cd}_{V,\mu} - j^{dc}_{V,\mu} | \phi^b(p_i) \rangle = \left(\delta^{ac}\delta^{db} - \delta^{ad}\delta^{bc} \right) i(p_f + p_i)_\mu F_V \left[(p_f - p_i)^2 \right] . \quad (18)$$

The procedure to find the leading logarithm for this observable follows the lines of the one for the decay constant. For the wave function renormalization one may again use the results obtained in the mass calculation. We express here the results in terms of $\tilde{t} = t/M_\pi^2$ and

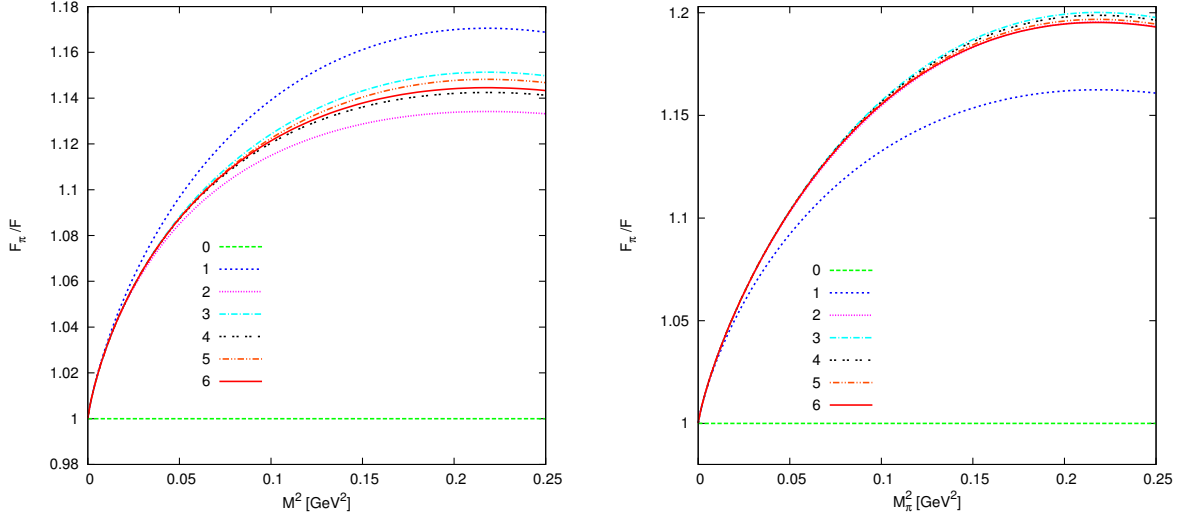$$L_\mathcal{M} = \frac{M_\pi^2}{16\pi^2 F_\pi^2} \log \frac{\mu^2}{\mathcal{M}^2} \quad (19)$$

9

Figure 2: The contribution of the leading logarithms to F_π/F order by order for $\mu = 0.77$ GeV and $N = 3$. The left panel shows the expansion in L with $F = 0.090$ GeV fixed, the right panel the expansion in L_{phys} with $F_\pi = 0.0922$ MeV fixed.

with a scale $\mathcal{M}^2$ that is some combination of t and M_π^2. Again we have added one more order compared to the result in [7]. To fifth order we find

$$
\begin{aligned}
F_V(t) = 1 &+ L_{\mathcal{M}}\Big[1/6\,\tilde{t}\Big] + L_{\mathcal{M}}^2\Big[\tilde{t}\,(-11/12 + 5/12\,N) + \tilde{t}^2\,(5/36 - 1/24\,N)\Big] \\
&+ L_{\mathcal{M}}^3\Big[\tilde{t}\,(+1387/648 - 845/324\,N + 7/9\,N^2) + \tilde{t}^2\,(-4007/6480 \\
&\quad + 3521/6480\,N - 29/180\,N^2) + \tilde{t}^3\,(+721/12960 - 47/1440\,N + 1/80\,N^2)\Big] \\
&+ L_{\mathcal{M}}^4\Big[\tilde{t}\,(-44249/15552 + 222085/31104\,N - 55063/10368\,N^2 + 127/96\,N^3) \\
&\quad + \tilde{t}^2\,(+349403/155520 - 15139/4860\,N + 86719/51840\,N^2 - 199/480\,N^3) \\
&\quad + \tilde{t}^3\,(-85141/155520 + 885319/1555200\,N - 5303/19200\,N^2 + 21/320\,N^3) \\
&\quad + \tilde{t}^4\,(+4429/103680 - 57451/1555200\,N + 289/14400\,N^2 - 1/240\,N^3)\Big] \\
&+ L_{\mathcal{M}}^5\Big[\tilde{t}\,(-2278099/777600 - 2377637/466560\,N + 64763783/4665600\,N^2 \\
&\quad - 178063/19200\,N^3 + 69/32\,N^4) + \tilde{t}^2\,(-62212433/11664000 \\
&\quad + 27685279/2332800\,N - 376597697/38880000\,N^2 \\
&\quad + 53519593/12960000\,N^3 - 361/400\,N^4) + \tilde{t}^3\,(74033879/30240000 \\
&\quad - 2247054421/544320000\,N + 32125153/11340000\,N^2 \\
&\quad - 13264877/12096000\,N^3 + 1209/5600\,N^4) + \tilde{t}^4\,(-299603257/816480000 \\
&\quad + 213192107/408240000\,N - 98330371/272160000\,N^2 \\
&\quad + 546331/3780000\,N^3 - 233/8400\,N^4) + \tilde{t}^5\,(3090331/163296000
\end{aligned}
$$

$$- 36097349/1632960000\,N + 28441883/1632960000\,N^2$$
$$- 15971/2268000\,N^3 + 1/672\,N^4\big)\Big]. \tag{20}$$

Note that $F_V(0) = 1$ as it should be.

The vector form factor was also calculated in the massless case in [4]. In order to transform our result into this limit, we define

$$K_t \equiv \frac{t}{16\pi^2 F^2} \log\left(-\frac{\mu^2}{t}\right). \tag{21}$$

Replacing $\mathcal{M}^2 \to t$ and then performing the limit $M_\pi^2 \to 0$ (which implies $F_\pi \to F$), we get

$$
\begin{aligned}
F_V^0(t) = {} & 1 + K_t/6 + K_t^2(5/36 - N/24) \\
& + K_t^3(721/12960 - 47/1440\,N + N^2/80) \\
& + K_t^4(4429/103680 - 57451/1555200\,N + 289/14400\,N^2 - N^3/240) \\
& + K_t^5(3090331/163296000 - 36097349/1632960000\,N \\
& \quad + 28441883/1632960000\,N^2 - 15971/2268000\,N^3 + N^4/672).
\end{aligned}
\tag{22}
$$

This differs from the result of [4]. The difference is discussed in the appendix using a dispersive approach as an alternative check, which agrees with [7] and (22). Up to the given order, the coefficient of the highest power in N in (22) at each order is of the form

$$f_V^n = \frac{(-1)^{n-1}}{(n+1)(n+2)}\left(\frac{N}{2}\right)^{n-1}, \tag{23}$$

such that, assuming this representation of f_V^n to be valid also at higher orders, we can write

$$F_V^0(t) = 1 + \sum_{n=1}^{\infty} f_V^n K_t^n (1 + O(1/N)). \tag{24}$$

The summation can be performed explicitly and we obtain the next-to-large N result in the chiral limit in a closed form:

$$F_V^{0NLN}(t) = 1 + \frac{1}{N} + \frac{4}{K_t N^2}\left[1 - \left(1 + \frac{2}{K_t N}\right)\log\left(1 + \frac{K_t N}{2}\right)\right]. \tag{25}$$

These large N formulas are also present in [4] up to a sign mistake. In that article, the large N has been explicitly calculated to all orders.

We close this section with giving the expansion for the radius and curvature of the vector form factor defined by

$$F_V(t) = 1 + \frac{1}{6}\langle r^2 \rangle_V t + c_V t^2 + \dots. \tag{26}$$

The coefficients c_i for the expansion in physical quantities are given in Tables 5 and 6 in units of M_π^2, again adding one order compared to [7]. The result up to two-loop order agrees with the LL extracted from the full two-loop calculation [21]. We do not present numerical results for the vector form factor since these are dominated in the physical case $N = 3$ by the large higher-order coefficient contributions, see, e.g., [8, 21].

i	c_i for $N = 3$	c_i for general N
1	1	1
2	2	$-11/2 + 5/2\,N$
3	853/108	$1387/108 - 845/54\,N + 14/3\,N^2$
4	50513/1296	$-44249/2592 + 222085/5184\,N - 55063/1728\,N^2 + 127/16\,N^3$
5	120401/648	$-2278099/129600 - 2377637/77760\,N + 64763783/777600\,N^2$ $-178063/3200\,N^3 + 207/16\,N^4$

Table 5: The coefficients c_i of the leading logarithm L_{phys} in the expansion of the radius $\langle r^2 \rangle_V$ in the case $N = 3$ and for general N.

i	c_i for $N = 3$	c_i for general N
1	0	0
2	1/72	$5/36 - 1/24\,N$
3	$-71/162$	$-4007/6480 + 3521/6480\,N - 29/180\,N^2$
4	$-25169/7776$	$349403/155520 - 15139/4860\,N + 86719/51840\,N^2 - 199/480\,N^3$
5	$-1349303/72900$	$-62212433/11664000 + 27685279/2332800\,N$ $-376597697/38880000\,N^2 + 53519593/12960000\,N^3 - 361/400\,N^4$

Table 6: The coefficients c_i of the leading logarithm L_{phys} in the expansion of the curvature c_V in the case $N = 3$ and for general N.

4 Leading logarithms in the anomalous sector

4.1 $\pi\gamma \to \pi\pi$

The process $\pi^0\gamma \to \pi^0\pi^0$ is forbidden by C-symmetry and we will therefore concentrate on $\pi^-\gamma \to \pi^-\pi^0$. The latter can be represented by the anomalous $VAAA$ quadrangle diagram at quark level. We follow the notation introduced in [22] where the one-loop order was calculated. At tree-level, the amplitude for $\pi^-(p_1)\gamma(k) \to \pi^-(p_2)\pi^0(p_0)$ can be obtained from the Wess-Zumino-Witten Lagrangian (6):

$$A_0 = \frac{ie}{4\pi^2 F^3}\epsilon_{\mu\nu\alpha\beta}\varepsilon^\mu(k)p_1^\nu p_2^\alpha p_0^\beta \,. \tag{27}$$

For higher orders we express the results in terms of physical variables only as

$$A = iF^{3\pi}(s, t, u)\epsilon_{\mu\nu\alpha\beta}\varepsilon^\mu(k)p_1^\nu p_2^\alpha p_0^\beta \,, \tag{28}$$

with the Mandelstam variables

$$s = (p_1 + k)^2, \quad t = (p_1 - p_2)^2, \quad u = (p_1 - p_0)^2, \quad s + t + u = 3M_\pi^2 + k^2 \,. \tag{29}$$
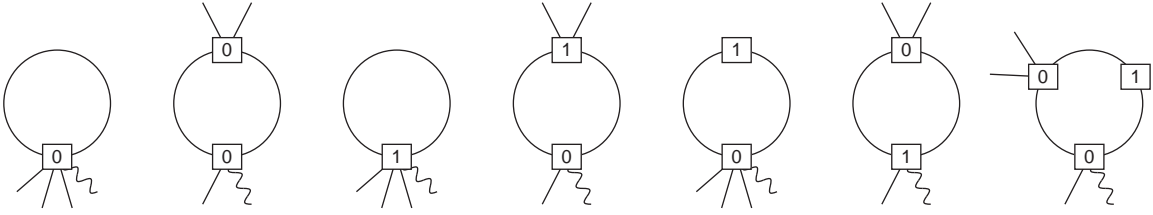
Figure 3: The irreducible diagrams for the process $\pi\gamma \to \pi\pi$ up to two-loop level. The first two diagrams are the one-loop level.

The function $F^{3\pi}(s,t,u)$ for $\gamma\pi \to \pi\pi$ is fully symmetric in s, t, u. We write it in terms of F_π as

$$F^{3\pi}(s,t,u) = F_0^{3\pi} f(s,t,u), \quad F_0^{3\pi} = \frac{e}{4\pi^2 F_\pi^3}. \tag{30}$$

If one expands $f(s,t,u)$ as a polynomial in s, t, u one can use the relation in (29) to see how many new independent kinematical quantities can appear at each order. Up to fifth order in s, t, u there is only one at each order. At sixth order there are two. For the first five orders we choose as independent quantities[3]

$$\Delta_n = s^n + t^n + u^n. \tag{31}$$

We also define $\tilde{k}^2 = k^2/M_\pi^2$ and $\tilde{\Delta}_n = \Delta_n/M_\pi^{2n}$. In the end we write $f(s,t,u)$ in terms of $\tilde{k}^2, M_\pi^2, \tilde{\Delta}_2, \ldots, \tilde{\Delta}_5$.

The main focus of this article is calculating the leading logarithms in the anomalous sector. The procedure follows very similar steps as in the even sector. From the even sector we will need the wave function renormalization and the expressions for the higher-order purely mesonic vertices as well as the decay constant and mass when using an expansion in terms of physical quantities. Vertices coupling an even number of pions to a single photon are not needed at this point, because the two-flavour anomaly does not contain interaction terms involving an odd number of pions and no photon. What remains to be calculated are the irreducible diagrams with three external pions and one external photon. The required diagrams up to two-loop order are depicted in Fig. 3. As in Section 3, a box with n inside, $\boxed{n}$, means a vertex of order n. To reach the one-loop level, we must calculate the first two of these diagrams. Inspection of the remaining diagrams for the two-loop level shows that all vertices are already known except the one with five pions and one photon in the third diagram. The diagrams that are needed in order to obtain its divergence are shown in Fig. 4. Note that the vertex with three pions and one photon in the sixth diagram of Fig. 3 is fixed by the one-loop calculation, the first two diagrams in the same figure.

To go to higher orders we rapidly need vertices with many more legs. We have generated all diagrams needed and calculated them up to fifth order. We agree with the logarithm

---

[3]The same arguments can be applied to any process fully symmetric in s, t, and u. A prominent example is $\eta \to 3\pi^0$, where $s + t + u = 3M_\pi^2 + M_\eta^2$.
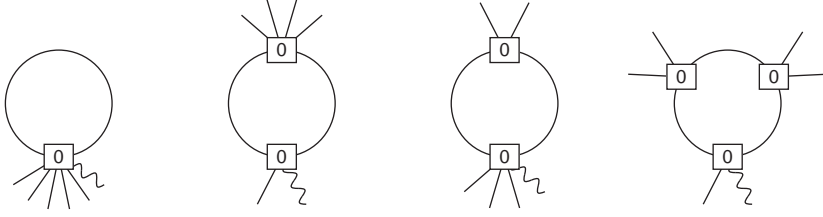
Figure 4: The irreducible (auxiliary) diagrams needed for the vertex $5\pi\gamma$ up to one-loop level.

determined from the full one-loop result [22]. The results were obtained in several different parametrizations with consistent results.

We have calculated the amplitude for $\pi^-\gamma \to \pi^-\pi^0$ up to five-loop level. In the general case, i.e., for $k^2, M_\pi^2 \neq 0$, we obtain

$$
\begin{aligned}
f^{LL}(s,t,u) = {} & 1 + L_\mathcal{M}\frac{1}{6}\left(3 + \tilde{k}^2\right) + L_\mathcal{M}^2\frac{1}{72}(\tilde{k}^2 - 3)(\tilde{k}^2 + 33) \\
& + L_\mathcal{M}^3\frac{1}{1296}\left(90\tilde{\Delta}_3 - 640\tilde{\Delta}_2 - 8157 + 2105\tilde{k}^2 + 81\tilde{k}^4 + \tilde{k}^6\right) + L_\mathcal{M}^4\frac{1}{155520}\Big[-1532\tilde{\Delta}_4 \\
& + \tilde{\Delta}_3(88538 + 1890\tilde{k}^2) - \tilde{\Delta}_2(577760 + 12240\tilde{k}^2 + 540\tilde{k}^4) - 2433375 + 1296190\tilde{k}^2 \\
& + 57430\tilde{k}^4 + 480\tilde{k}^6 + 185\tilde{k}^8\Big] + L_\mathcal{M}^5\frac{1}{326592000}\Big[\tilde{\Delta}_5(13252156) \\
& - \tilde{\Delta}_4(160744570 + 518350\tilde{k}^2) + \tilde{\Delta}_3(1465187530 + 39593272\tilde{k}^2 + 247260\tilde{k}^4) \\
& - \tilde{\Delta}_2(6756522937 + 257781206\tilde{k}^2 + 11188776\tilde{k}^4 - 9160\tilde{k}^6) - 6498695163 \\
& + 12675091794\tilde{k}^2 + 801259373\tilde{k}^4 + 4780240\tilde{k}^6 + 2948600\tilde{k}^8 - 1832\tilde{k}^{10}\Big].
\end{aligned}
\tag{32}
$$

The symmetry in s, t and u is obvious in this expression. Note that at second order $\tilde{\Delta}_2$ does not appear even though it could be present a priori.

We can check whether we find a simpler expression in the massless limit and for an on-shell photon, $k^2 = 0$. In this case we need to express the result in terms of the logarithm

$$
L_\Delta = \frac{1}{16\pi^2 F^2} \log\left(\frac{\mu^2}{\hat{\Delta}}\right),
\tag{33}
$$

where $\hat{\Delta}$ is some combination of s, t, and u:

$$
f^{LL0}(s,t,u) = 1 + \frac{5}{72}\Delta_3 L_\Delta^3 - \frac{383}{19440}\Delta_4 L_\Delta^4 + \frac{3313039}{81648000}\Delta_5 L_\Delta^5.
\tag{34}
$$

It is clear from symmetry considerations that there should be no term linear in L_Δ. We do however not know why the quadratic term is also absent.
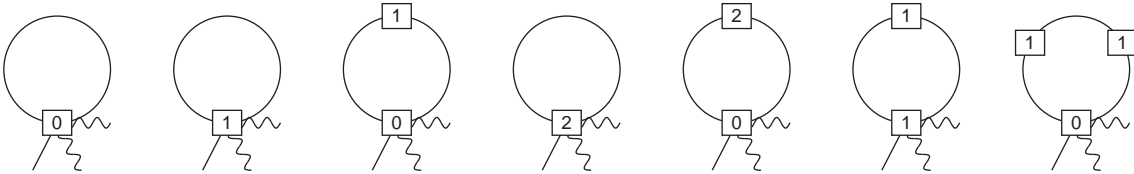
14

Figure 5: First type of the irreducible diagrams contributed to $\pi^0 \to \gamma\gamma$ up to three-loop order

4.2 $\pi^0 \to \gamma\gamma$

This is the most important process in the odd-intrinsic parity sector of QCD, since it is the process in which the chiral anomaly was discovered. It remains the main experimental test thereof.

We started our discussion of anomalous processes with $\pi\gamma \to \pi\pi$ because the leading logarithms for this process could be calculated from our results in the even intrinsic parity sector and just one type of anomalous vertex.

We define the reduced amplitude $F_{\pi\gamma\gamma}$ for $\pi^0 \to \gamma(k_1)\gamma(k_2)$

$$A = \epsilon_{\mu\nu\alpha\beta}\, \varepsilon_1^{*\mu}(k_1)\varepsilon_2^{*\nu}(k_2)\, k_1^\alpha k_2^\beta\, F_{\pi\gamma\gamma}(k_1^2, k_2^2)\,. \tag{35}$$

$F_{\pi\gamma\gamma}(k_1^2, k_2^2)$ is symmetric under the interchange of the two photons.

The irreducible diagrams contributing to $\pi^0 \to \gamma\gamma$ consist of two different types of one-loop diagrams. The first type contains the diagrams where both photons are attached to the *same* vertex, while in the diagrams of the second type, the two photons connect to two different vertices, only one of which is anomalous. We show here the diagrams needed for the calculation of the leading logarithms up to third order. Those of the first type are depicted in Fig. 5. There is one diagram at one-loop order, there are two at two-loop order, and four at three-loop order. The diagrams of the second type are depicted in Fig. 6. This time, there is one diagram at one-loop order, there are three at two-loop, and eight at three-loop order. The figures do not contain the auxiliary diagrams that are needed in order to determine the higher-order vertices with more than one pion leg. We only mention that up to three-loop order, one needs to calculate 11 and 23 diagrams for the first and second type of topologies, respectively.

The first type of diagrams is a consistent subset if we only keep the terms with two vector sources in the Lagrangian (6). That this leads to identical results for several different parametrizations provides a thorough check on the correctness of our programs for this class of diagrams separately.

We write the result with $\tilde{k}_i^2 = k_i^2/M_\pi^2$ in the form

$$F_{\pi\gamma\gamma}(k_1^2, k_2^2) = \frac{e^2}{4\pi^2 F_\pi} F_\gamma(k_1^2) F_\gamma(k_2^2) F_{\gamma\gamma}(k_1^2, k_2^2)\hat{F}\,. \tag{36}$$
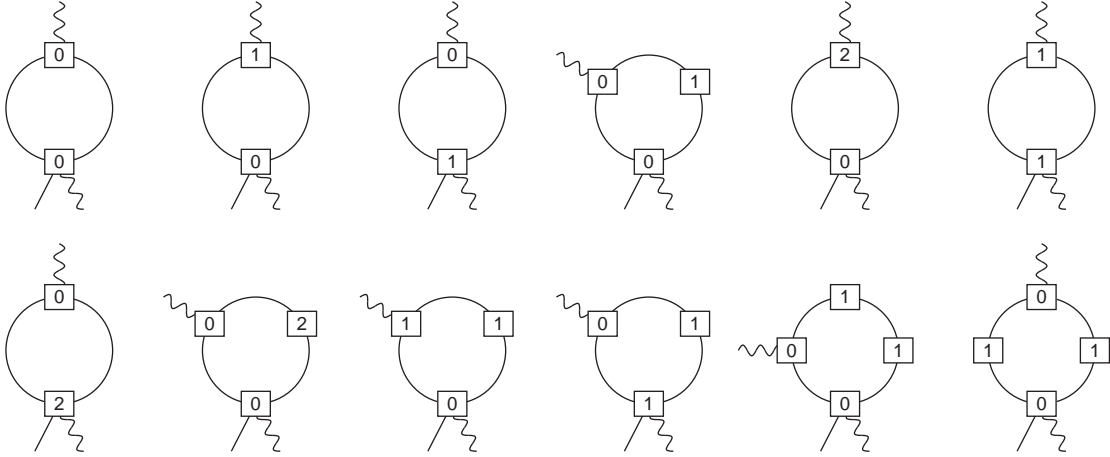
15

Figure 6: Second type of the irreducible diagrams contributed to $\pi^0 \to \gamma\gamma$ up to three-loop order

The functions $F_\gamma(k_i^2)$ and $F_{\gamma\gamma}(k_1^2, k_2^2)$ are defined to be equal to one for $k_i^2 = 0$. $F_{\gamma\gamma}(k_1^2, k_2^2)$ contains only those parts that cannot be absorbed in the F_γ and thus gives the part that cannot be obtained as a product of single photon form factors. Finally $\hat{F}$ gives the corrections for the on-shell decay $\pi^0 \to \gamma\gamma$.

We have calculated all contributions needed for the LLs up to six-loop order and obtained

$$
\begin{aligned}
\hat{F} = {} & 1 - 1/6\, L_{\mathcal{M}}^2 + 5/6\, L_{\mathcal{M}}^3 + 56147/7776\, L_{\mathcal{M}}^4 + 446502199/11664000\, L_{\mathcal{M}}^5 \\
& + 65694012997/367416000\, L_{\mathcal{M}}^6 \,,
\end{aligned}
$$

$$
\begin{aligned}
F_\gamma(k^2) = {} & 1 + L_{\mathcal{M}}(1/6\,\tilde{k}^2) + L_{\mathcal{M}}^2(5/24\,\tilde{k}^2 + 1/72\,\tilde{k}^4) + L_{\mathcal{M}}^3(71/432\,\tilde{k}^2 + 1/24\,\tilde{k}^4 \\
& + 1/1296\,\tilde{k}^6) + L_{\mathcal{M}}^4(-24353/31104\,\tilde{k}^2 + 4873/10368\,\tilde{k}^4 - 2357/31104\,\tilde{k}^6 \\
& + 145/31104\,\tilde{k}^8) + L_{\mathcal{M}}^5(-548440741/81648000\,\tilde{k}^2 + 9793363/3024000\,\tilde{k}^4 \\
& - 32952389/54432000\,\tilde{k}^6 + 487493/13608000\,\tilde{k}^8 - 2069/10886400\,\tilde{k}^{10}) \\
& + L_{\mathcal{M}}^6(-3519465627493/102876480000\,\tilde{k}^2 \\
& + 3560724235307/205752960000\,\tilde{k}^4 - 1524042680197/411505920000\,\tilde{k}^6 \\
& + 4741599089/11757312000\,\tilde{k}^8 - 510932327/13716864000\,\tilde{k}^{10} \\
& + 1775869/914457600\,\tilde{k}^{12}) \,,
\end{aligned}
$$

$$
\begin{aligned}
F_{\gamma\gamma}(k_1^2, k_2^2) = {} & 1 + L_{\mathcal{M}}^3\,\tilde{k}_1^2\tilde{k}_2^2\frac{1}{72} + L_{\mathcal{M}}^4\,\tilde{k}_1^2\tilde{k}_2^2\big[-203/7776 + 29/10368\,(\tilde{k}_1^2 + \tilde{k}_2^2) \\
& + 1/216\,(\tilde{k}_1^4 + \tilde{k}_2^4) - 1/144\,\tilde{k}_1^2\tilde{k}_2^2\big] + L_{\mathcal{M}}^5\,\tilde{k}_1^2\tilde{k}_2^2\big[-5983633/10206000 \\
& + 46103/1632960\,(\tilde{k}_1^2 + \tilde{k}_2^2) + 372113/11664000\,(\tilde{k}_1^4 + \tilde{k}_2^4) \\
& - 211/5443200\,(\tilde{k}_1^6 + \tilde{k}_2^6) - 394157/9072000\,\tilde{k}_1^2\tilde{k}_2^2 - 4/25515\,\tilde{k}_1^2\tilde{k}_2^2(\tilde{k}_1^2 + \tilde{k}_2^2)\big]
\end{aligned}
$$

16

$$+ L_{\mathcal{M}}^6 \tilde{k}_1^2 \tilde{k}_2^2 \big[- 1072421939773/205752960000$$

$$+ 1444445383/6531840000 \, (\tilde{k}_1^2 + \tilde{k}_2^2) + 10840553807/102876480000 \, (\tilde{k}_1^4 + \tilde{k}_2^4)$$

$$+ 282016297/205752960000 \, (\tilde{k}_1^6 + \tilde{k}_2^6) + 6157391/4115059200 \, (\tilde{k}_1^8 + \tilde{k}_2^8)$$

$$- 3852620057/29393280000 \, \tilde{k}_1^2 \tilde{k}_2^2 - 154739/58320000 \, \tilde{k}_1^2 \tilde{k}_2^2 (\tilde{k}_1^2 + \tilde{k}_2^2)$$

$$- 75041473/20575296000 \, \tilde{k}_1^2 \tilde{k}_2^2 (\tilde{k}_1^4 + \tilde{k}_2^4) + 174329/35721000 \, \tilde{k}_1^4 \tilde{k}_2^4 \big] . \tag{37}$$

The absence of the linear term in $\hat{F}$ agrees with the statement from [23, 24] that the contribution from one-loop diagrams at NLO can be absorbed into F_π. The quadratic term also coincides with the two-loop calculation of [25] and the complete one-loop expression for off-shell photons is the same as in [24].

Note that the nonfactorizable contribution $F_{\gamma\gamma}$ only starts at three-loop order and that the part surviving in the chiral limit only starts at four-loop level. The leading logarithms thus predict this part to be fairly small.

The lowest-order results for the two anomalous processes are connected via the current algebra relation [26, 27]

$$F^{3\pi}(0,0,0) = \frac{1}{eF_\pi^2} F_{\pi\gamma\gamma}(0,0) , \tag{38}$$

which holds exactly in the chiral limit. Even beyond this limit it is valid also at the one-loop level for the leading logarithms as can be seen by comparing (32) and (37). The current algebra relation remains true, if in both amplitudes one of the photons is allowed to be off-shell, i.e.

$$F^{3\pi}(s,t,u)\Big|_{s+t+u=3M_\pi^2+k^2} = \frac{1}{eF_\pi^2} F_{\pi\gamma\gamma}(k^2,0) . \tag{39}$$

It turns out that in the chiral limit, this relation holds for the leading logarithms up to two loops, as can again be checked from (32) and (37).

5 Phenomenology of the anomalous sector

5.1 $\pi\gamma \to \pi\pi$

The only direct measurement of the $\pi\gamma \to \pi\pi$ vertex has been performed at the IHEP accelerator in Serpukhov [28] using $\pi^-\gamma \to \pi^-\pi^0$, where the γ comes from the electromagnetic field of a nucleus via the Primakoff effect. The relevant cross-section was measured with a pion beam of $E = 40$ GeV and the photons' virtuality was in the region $k^2 < 2\times10^{-3}$ GeV^2, which can be neglected at the present precision. The analysis is for values of $s < 10M_\pi^2$ and thus within the region where ChPT is applicable. Assuming the function $F^{3\pi}(s,t,u)$ of (30) to be approximately constant, $F^{3\pi}(s,t,u) \approx \bar{F}^{3\pi}$, they find

$$\bar{F}^{3\pi}_{\text{exp}} = 12.9 \pm 0.9 \pm 0.5 \text{ GeV}^{-3} . \tag{40}$$

Another derivation used the data on $\pi^- e^- \to \pi^- e^- \pi^0$ [29] to determine $F_0^{3\pi}$ [30]. They obtained

$$F_{0,\text{exp}}^{3\pi} = 9.9 \pm 1.1 \text{ GeV}^{-3} \quad \text{or} \quad 9.6 \pm 1.1 \text{ GeV}^{-3} , \tag{41}$$

depending on the way electromagnetic corrections are included.

The value in (40) needs to be corrected for extrapolation to the point $s = t = u = 0$. The one-loop ChPT corrections were evaluated in [22] and a possibly large electromagnetic correction identified in [31]. The main conclusion is that the experimental values are in fairly good agreement with the theoretical result of (30) which gives $F_0^{3\pi} = 9.8 \text{ GeV}^{-3}$ as discussed further below.

The comparison with [28] goes via their result $\sigma/Z^2 = 1.63 \pm 0.23 \pm 0.13$ nb and [28, 31]

$$\frac{\sigma}{Z^2} = \frac{\alpha}{\pi} \int_{4M_\pi^2}^{10M_\pi^2} ds \left(\ln \frac{q_{\max}^2}{q_{\min}^2} + \frac{q_{\min}^2}{q_{\max}^2} - 1 \right) \frac{\sigma_{\gamma\pi \to \pi\pi}}{s - M_\pi^2} ,$$

$$\sigma_{\gamma\pi \to \pi\pi} = \frac{1}{1024\pi} s(s - M_\pi^2) \left(1 - \frac{4M_\pi^2}{s} \right)^{3/2} \int_0^\pi d\theta \sin^3 \theta \left| F_0^{3\pi} f(s, t, u) \right|^2 . \tag{42}$$

Inserting the charged pion mass, $q_{\max}^2 = 2 \cdot 10^{-3} \text{ GeV}^2$, $q_{\min}^2 = ((s - M_\pi^2)/(2E))^2$, and $f(s, t, u) = 1$ in (42) leads to the value in (40).

The various known higher-order corrections can now be included via $f(s, t, u)$:

$$f(s, t, u) = 1 + f_0^{\text{EM}} + f_1^{\text{loop}} + f_1^{\text{tree}} + \dots . \tag{43}$$

The dependence on s, t, u is tacitly assumed for all functions f_i. The index i refers to the $\hbar$ order. The leading-order electromagnetic correction f_0^{EM} was determined in [31] as $f_0^{\text{EM}} = -2e^2 F_\pi^2/t$ and higher-order electromagnetic corrections were found to be small. The next-to-leading-order correction coming from one-loop graphs is, in the isospin limit, given by [22]

$$f_1^{\text{loop}} = \frac{1}{6F_\pi^2} \left[-\frac{M_\pi^2}{(4\pi)^2} \left(1 + 3 \log \frac{M_\pi^2}{\mu^2} \right) + I(s) + I(t) + I(u) \right] , \tag{44}$$

with $I(s) = (s - 4M_\pi^2)\bar{J}(s)$, where $\bar{J}(s)$ is the standard subtracted two-point function

$$16\pi^2 \bar{J}(q^2) = \sigma \log \frac{\sigma - 1}{\sigma + 1} + 2 , \qquad \sigma = \sqrt{1 - 4M_\pi^2/q^2} . \tag{45}$$

The logarithmic term in (44) agrees with our LL calculation. The full expression accounting for the pion mass difference can be found in [31].

The contribution from the NLO Lagrangian can be expressed in terms of the low-energy constants introduced in [32] as

$$f_1^{\text{tree}} = 128\pi^2 M_\pi^2 \left(c_2^{Wr} + c_6^{Wr} \right) . \tag{46}$$

18

	LO	f_0^{EM}	f_1^{loop}(LL)	f_1^{loop}	f_1^{tree} (HLS)	f_1^{tree} (CQM)	f_1^{tree} (SDE)
$F_0^{3\pi}$	12.9	12.3	12.0	11.9	11.4	10.1	12.0

Table 7: The extraction of the anomalous $\gamma 3\pi$ factor $F_0^{3\pi}$ (in GeV^{-3}) from experiment using various estimates of the higher-order corrections. LO includes no higher-order corrections and thus coincides with (40). The next column contains the QED correction f_0^{EM}. Then come the values including in addition the leading logarithm and the complete correction from f_1^{loop}. The last three columns also contain f_1^{tree} using the model estimates in (47).

In order to estimate the value of f_1^{tree}, several methods exist in the literature: hidden local symmetry (HLS) [22], phenomenology [33], the constituent quark model (CQM) [33, 34], Schwinger-Dyson equation (SDE) [35], or resonance saturation [36], to name a few. The spread in results can be seen from the estimates following from three of these methods

$$f_1^{\text{tree}} = \frac{3M_\pi^2}{2M_\rho^2} = 0.048 \text{ (HLS)}, \qquad = 0.19 \text{ (CQM)}, \qquad = -0.01 \text{ (SDE)}. \qquad (47)$$

The two-loop corrections, estimated using dispersive techniques [37], are found to be small.

These corrections can now be incorporated in the calculation of $F_0^{3\pi}$ from the cross section measured at Serpukhov using (42). Turning them on one by one, we find the results listed in Table 7. Comparison of the third and fourth column shows that at the one-loop order, the leading logarithm provides a good estimate for the size of the complete correction: it accounts for 60% of the shift. The uncertainty on the listed values has two main sources: the experimental uncertainty of about ± 1 GeV^{-3} and the model dependence of the c_i^{Wr}. From the spread of the estimates in Table 7, the latter also is about ± 1 GeV^{-3}. The total error, adding quadratically, is thus about ± 1.5 GeV^{-3}, such that the theoretical result $F_0^{3\pi} = 9.8$ GeV^{-3} agrees reasonably with the final values at the one-loop level.

Let us now return to the discussion of the expansion f^{LL} in (32). The one-loop LL shifts the result by -0.3 as already shown. Adding the LL up contributions up to five-loop order in (42) leads to

$$F_0^{3\pi LL} = (12.9 - 0.3 + 0.04 + 0.02 + 0.006 + 0.001 + \ldots) \text{ GeV}^{-3}. \qquad (48)$$

Clearly, the series converges rather well. The small size of the LLs beyond one loop indicates that the full corrections at higher orders are negligible.

The total cross section obtained from only the LL contributions as a function of the center-of-mass energy is depicted in Fig. 7.

5.2 $\pi^0 \to \gamma\gamma$

For the decay $\pi^0 \to \gamma\gamma$, there is more experimental information available. For a recent review, see [38]. The current PDG average ([39], updated 2011) for the lifetime of the neutral pion is based on six experiments: three relying on the Primakoff effect [40–42], a
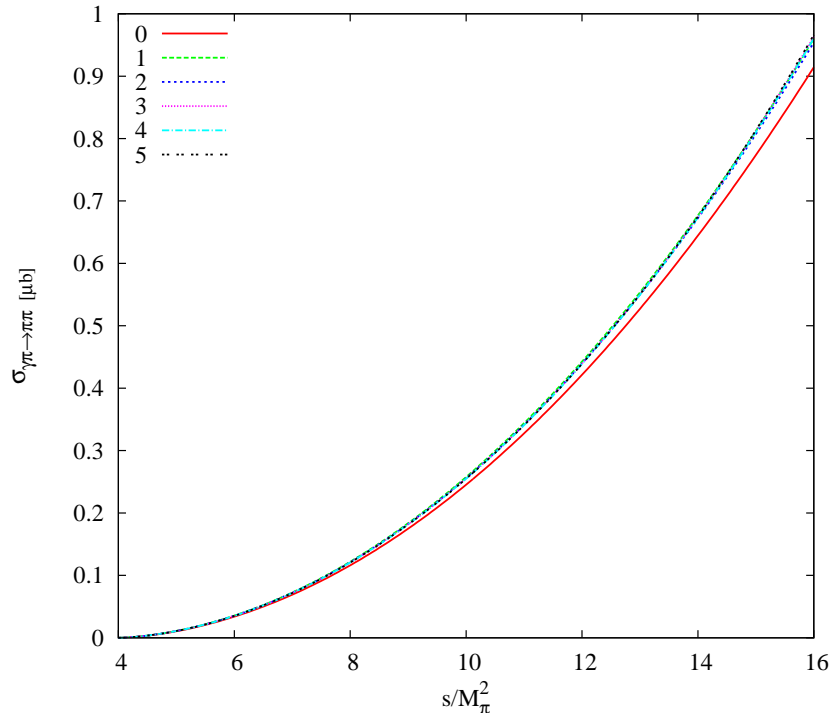
Figure 7: The leading logarithm contribution to the total cross section for $\pi^- \gamma \to \pi^- \pi^0$ as a function of s.

direct measurement [43], an $e^+ e^-$ collider measurement [44], and a measurement of the weak form factor in $\pi^+ \to e^+ \nu \gamma$ [45], which is related to the π^0 lifetime via the conserved vector current hypothesis. This leads to the average lifetime $\tau_{\pi^0} = (8.4 \pm 0.4) \times 10^{-17} s$. Including the recent precise measurement by PrimEx at JLab [46],

$$\Gamma(\pi^0 \to \gamma\gamma)_{\text{PrimEx}} = 7.82 \pm 0.14 \pm 0.17 \, \text{eV} \,, \tag{49}$$

leads to a smaller uncertainty, $\tau_{\pi^0} = (8.35 \pm 0.31) \times 10^{-17} s$. Ongoing efforts by the PrimEx collaboration are expected to decrease the error by a factor two.

The partial decay width is related to the decay amplitude by

$$\Gamma_{\gamma\gamma} = \frac{M_\pi^3}{64\pi} |F_{\pi\gamma\gamma}|^2 \,. \tag{50}$$

At lowest order we find from the Wess-Zumino-Witten Lagrangian

$$F_{\pi\gamma\gamma}^{\text{LO}} = \frac{e^2}{4\pi^2 F_\pi} \quad \Rightarrow \quad \Gamma(\pi^0 \to \gamma\gamma)_{\text{LO}} \approx 7.76 \, \text{eV} \,, \tag{51}$$

which is in perfect agreement with the PDG average as well as with the PrimEx result (49). Higher-order corrections might still destroy the agreement and we can use the leading

20

logarithms to estimate the size of these contributions and to examine the convergence of the chiral series. Notice that no chiral logarithms are present at the one-loop level once everything is expressed in terms of the physical quantities F_π and M_π [23, 24]. At the two-loop level, leading logarithms start to contribute [25]. At present the best prediction including electromagnetic and two-loop effects is [25]

$$\Gamma_{\pi^0 \to \gamma\gamma} = (8.09 \pm 0.11)\,\text{eV}\,, \qquad (52)$$

which leads to the lifetime $\tau_{\pi^0} = (8.04 \pm 0.11)\,10^{-17}\,\text{s}$.

Our result for $\hat{F}$ in (37) indicates that the convergence is fast and higher orders are small. Putting in $\mu = 0.77$ GeV we obtain

$$\hat{F} = 1 + 0 - 0.000372 + 0.000088 + 0.000036 + 0.000009 + 0.0000002 + \ldots\,, \qquad (53)$$

which clearly shows a fast convergence.

We now turn to the discussion of the meson-photon transition form factor $F_\gamma(-Q^2)$, normalized to the value at $Q^2 = 0$, which has been given in (37). It was measured by CELLO [47], CLEO [48], and recently by BaBar [49] mainly in the range $1 \leq Q^2 \leq 40\,\text{GeV}^2$. New activity is expected for very low Q^2 by KLOE-2 at DAΦNE [50] which should directly test the prediction.

The LL contribution up to fifth order has been given in (37). Our result for the LL contribution to this quantity is depicted in Fig. 8 together with the VMD prediction

$$F_\gamma^{\text{VMD}}(-Q^2) = \frac{m_V^2}{m_V^2 + Q^2}\,. \qquad (54)$$

6 Conclusion

In this paper we have extended the earlier work on leading logarithms in effective field theories to the anomalous sector. First we improved the programs used in the earlier work on the massive nonlinear sigma model [6, 7]. This allowed us to compute one order higher than in those papers and we presented results for the mass, decay constant and the vector form factor. For the latter we clarified the discrepancy with the chiral limit work of [4] and we presented some numerical results as well.

The main part of this paper is the extension to the anomalous sector. We thus added the Wess-Zumino-Witten term to the massive nonlinear sigma model for $N = 3$ and computed the leading logarithms to six-loop order for $\pi^0 \to \gamma^*\gamma^*$ and five-loop order for the $\gamma^*\pi\pi\pi$ vertex. We did not find a simple guess for the coefficients which was one of the hopes when starting this work. In both cases the leading logarithms indicate that the chiral series converges fast and we presented some numerical results for the pion lifetime, the transition form factor and the $\gamma^*\pi\pi\pi$ vertex.
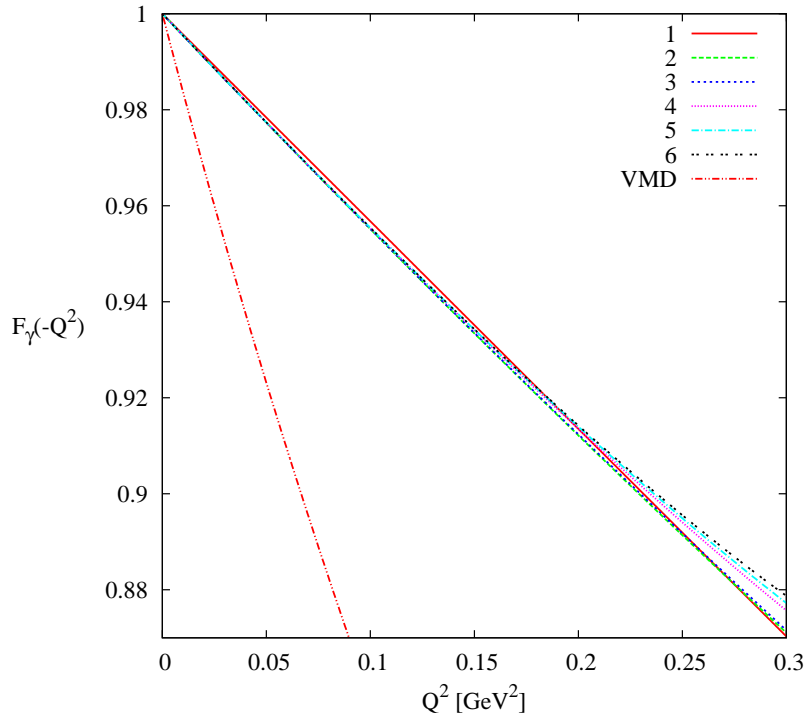
Figure 8: The LL contribution to $F_\gamma(-Q^2)$ at different orders. Also shown is the VMD prediction as a comparison.

Acknowledgments

A Dispersive approach for the pion form factor

Since the leading logarithms for the vector form factor in the chiral limit obtained in [7] and here do not agree with the corresponding result from Kivel et al. [4], another check of our result is in order. In [5], it was found that the partial wave amplitudes for $\pi\pi$ scattering are given by

$$t_l^I(s) = \frac{\pi}{2} \sum_{n=1}^{\infty} \omega_{nl}^I \frac{\hat{S}(s)^n}{2l+1} \ln^{n-1}\left(\frac{\mu^2}{s}\right) + \mathcal{O}(\text{NLL}), \tag{55}$$

22

with the dimensionless function $\hat{S}(s) = \frac{s}{(4\pi F)^2}$. The coefficients ω_{nl}^I can be found in Tables I and II in [5].

The leading logarithms for the scalar form factor are

$$F_S(s) = \sum_{n=0}^{\infty} f_n^S \hat{S}(s)^n \ln^n \left(-\frac{\mu^2}{s} \right) . \tag{56}$$

In this case, the results from [4] and [7] for the coefficients f_0^S are in agreement. The discontinuity across the cut of the scalar form factor must satisfy

$$\text{disc } F_S(s) = t_0^0 F_S(s) , \tag{57}$$

which can be easily verified to hold for the coefficients f_n^S given in [4, 7].

A similar expansion holds for the vector form factor:

$$F_V(s) = \sum_{n=0}^{\infty} f_n^V \hat{S}(s)^n \ln^n \left(-\frac{\mu^2}{s} \right) + \mathcal{O}(\text{NLL}) . \tag{58}$$

This time, however, the results from [4] disagree with ours and [7] for $n > 2$. The discontinuity across the cut of the vector form factor must hold

$$\text{disc } F_V(s) = t_1^1 F_V(s) , \tag{59}$$

which is only given for the f_n^V from us and [7]. We therefore conclude that this is the correct result.

Dropping the factor $(-1)^{p+1}$ in (12) of [4] brings that result in agreement with ours. That there is indeed a misprint in [4] was confirmed to us by the authors and was stated in the PhD thesis of A. A. Vladimirov.

References

[1] S. Weinberg, *Phenomenological Lagrangians*, *Physica* **A96** (1979) 327. Festschrift honoring Julian Schwinger on his 60th birthday.

[2] M. Büchler and G. Colangelo, *Renormalization group equations for effective field theories*, *Eur.Phys.J.* **C32** (2003) 427–442, [`hep-ph/0309049`].

[3] N. Kivel, M. Polyakov and A. Vladimirov, *Chiral logarithms in the massless limit tamed*, *Phys.Rev.Lett.* **101** (2008) 262001, [`arXiv:0809.3236`].

[4] N. Kivel, M. Polyakov and A. Vladimirov, *Leading chiral logarithms for pion form factors to arbitrary number of loops*, *JETP Lett.* **89** (2009) 529–534, [`arXiv:0904.3008`].

[5] J. Koschinski, M. V. Polyakov and A. A. Vladimirov, *Leading infrared logarithms from unitarity, analyticity and crossing*, Phys.Rev. **D82** (2010) 014014, [arXiv:1004.2197].

[6] J. Bijnens and L. Carloni, *Leading logarithms in the massive O(N) nonlinear sigma model*, Nucl.Phys. **B827** (2010) 237–255, [arXiv:0909.5086].

[7] J. Bijnens and L. Carloni, *The massive O(N) non-linear sigma model at high orders*, Nucl.Phys. **B843** (2011) 55–83, [arXiv:1008.3499].

[8] J. Gasser and H. Leutwyler, *Chiral perturbation theory to one loop*, Annals Phys. **158** (1984) 142.

[9] S. Weinberg, *Nonlinear realizations of chiral symmetry*, Phys.Rev. **166** (1968) 1568–1577.

[10] M. B. Einhorn, *Speculations on a strongly interacting Higgs sector*, Nucl.Phys. **B246** (1984) 75.

[11] F. Sannino, *Dynamical stabilization of the Fermi scale: Phase diagram of strongly coupled theories for (minimal) walking technicolor and unparticles*, arXiv:0804.0182.

[12] S. R. Coleman, J. Wess and B. Zumino, *Structure of phenomenological Lagrangians. 1.*, Phys.Rev. **177** (1969) 2239–2247.

[13] S. L. Adler, *Axial vector vertex in spinor electrodynamics*, Phys.Rev. **177** (1969) 2426–2438.

[14] S. L. Adler and W. A. Bardeen, *Absence of higher order corrections in the anomalous axial vector divergence equation*, Phys.Rev. **182** (1969) 1517–1536.

[15] W. A. Bardeen, *Anomalous Ward identities in spinor field theories*, Phys.Rev. **184** (1969) 1848–1857.

[16] J. Bell and R. Jackiw, *A PCAC puzzle: $\pi^0 \to \gamma\gamma$ in the sigma model*, Nuovo Cim. **A60** (1969) 47–61.

[17] J. Wess and B. Zumino, *Consequences of anomalous Ward identities*, Phys.Lett. **B37** (1971) 95.

[18] E. Witten, *Global aspects of current algebra*, Nucl.Phys. **B223** (1983) 422–432.

[19] R. Kaiser, *Anomalies and WZW term of two flavor QCD*, Phys.Rev. **D63** (2001) 076010, [hep-ph/0011377].

[20] J. Vermaseren, *New features of FORM*, math-ph/0010025.

[21] J. Bijnens, G. Colangelo and P. Talavera, *The vector and scalar form-factors of the pion to two loops*, *JHEP* **9805** (1998) 014, [`hep-ph/9805389`].

[22] J. Bijnens, A. Bramon and F. Cornet, *Three pseudoscalar photon interactions in chiral perturbation theory*, *Phys.Lett.* **B237** (1990) 488.

[23] J. Donoghue, B. R. Holstein and Y. Lin, *Chiral loops in π^0, $\eta^0 \to \gamma\gamma$ and η-η' mixing*, *Phys.Rev.Lett.* **55** (1985) 2766–2769.

[24] J. Bijnens, A. Bramon and F. Cornet, *Pseudoscalar decays into two photons in chiral perturbation theory*, *Phys.Rev.Lett.* **61** (1988) 1453.

[25] K. Kampf and B. Moussallam, *Chiral expansions of the π^0 lifetime*, *Phys.Rev.* **D79** (2009) 076005, [`arXiv:0901.4688`].

[26] S. L. Adler, B. W. Lee, S. Treiman and A. Zee, *Low-energy theorem for $\gamma + \gamma \to \pi + \pi + \pi$*, *Phys.Rev.* **D4** (1971) 3497–3501.

[27] M. Terent'ev, *Process $\pi^\pm \to \pi^0\pi^\pm$ in Coulomb field and anomalous divergence of neutral axial vector current*, *Phys.Lett.* **B38** (1972) 419.

[28] Y. Antipov, V. Batarin, V. Bezzubov, N. Budanov, Y. Gorin et. al., *Investigation of the chiral anomaly $\gamma \to 3\pi$ in pion pair production by pion in the nuclear Coulomb field*, *Phys.Rev.* **D36** (1987) 21.

[29] S. Amendolia, M. Arik, B. Badelek, G. Batignani, G. Beck et. al., *First measurement of the reaction $\pi^- e \to \pi^- \pi^0 e$*, *Phys.Lett.* **B155** (1985) 457.

[30] I. Giller, A. Ocherashvili, T. Ebertshauser, M. Moinester and S. Scherer, *A new determination of the $\gamma\pi \to \pi\pi$ anomalous amplitude via $\pi^- e^- \to \pi^- e^- \pi^0$ data*, *Eur.Phys.J.* **A25** (2005) 229–240, [`hep-ph/0503207`].

[31] L. Ametller, M. Knecht and P. Talavera, *Electromagnetic corrections to $\gamma\pi^\pm \to \pi^0\pi^\pm$*, *Phys.Rev.* **D64** (2001) 094009, [`hep-ph/0107127`].

[32] J. Bijnens, L. Girlanda and P. Talavera, *The anomalous chiral lagrangian of order p^6*, *Eur.Phys.J.* **C23** (2002) 539–544, [`hep-ph/0110400`].

[33] O. Strandberg, *Determination of the anomalous chiral coefficients of order p^6*, `hep-ph/0302064`. Masters Thesis (Advisor: Johan Bijnens).

[34] J. Bijnens, *The anomalous sector of the QCD effective lagrangian*, *Nucl.Phys.* **B367** (1991) 709–730.

[35] S.-Z. Jiang and Q. Wang, *Computation of the coefficients for p^6 order anomalous chiral Lagrangian*, *Phys.Rev.* **D81** (2010) 094037, [`arXiv:1001.0315`].

[36] K. Kampf and J. Novotny, *Resonance saturation in the odd-intrinsic parity sector of low-energy QCD*, *Phys.Rev.* **D84** (2011) 014036, [`arXiv:1104.3137`].

[37] T. Hannah, *The anomalous process $\gamma\pi \to \pi\pi$ to two loops*, *Nucl.Phys.* **B593** (2001) 577–595, [`hep-ph/0102213`].

[38] A. Bernstein and B. R. Holstein, *Neutral pion lifetime measurements and the QCD chiral anomaly*, `arXiv:1112.4809`.

[39] **Particle Data Group** Collaboration, K. Nakamura et. al., *Review of particle physics*, *J.Phys.G* **G37** (2010) 075021.

[40] V. Kryshkin, A. Sterligov and Y. Usov, *Measurement of lifetime of the π^0 meson*, *Zh.Eksp.Teor.Fiz.* **57** (1969) 1917–1922.

[41] G. Bellettini, C. Bemporad, P. Braccini, C. Bradaschia, L. Foa et. al., *A new measurement of the π^0 lifetime through the Primakoff effect in nuclei*, *Nuovo Cim.* **A66** (1970) 243–252.

[42] A. Browman, J. DeWire, B. Gittelman, K. Hanson, D. Larson et. al., *The decay width of the neutral π meson*, *Phys.Rev.Lett.* **33** (1974) 1400.

[43] H. Atherton, C. Bovet, P. Coet, R. Desalvo, N. Doble et. al., *Direct measurement of the lifetime of the neutral pion*, *Phys.Lett.* **B158** (1985) 81–84.

[44] **Crystal Ball** Collaboration, D. Williams et. al., *Formation of the pseudoscalars π^0, η and η' in the reaction $\gamma\gamma \to \gamma\gamma$*, *Phys.Rev.* **D38** (1988) 1365.

[45] M. Bychkov, D. Pocanic, B. VanDevender, V. Baranov, W. H. Bertl et. al., *New precise measurement of the pion weak form factors in $\pi^+ \to e^+\nu\gamma$ decay*, *Phys.Rev.Lett.* **103** (2009) 051802, [`arXiv:0804.1815`].

[46] **PrimEx** Collaboration, I. Larin et. al., *A new measurement of the π^0 radiative decay width*, *Phys.Rev.Lett.* **106** (2011) 162303, [`arXiv:1009.1681`].

[47] **CELLO** Collaboration, H. Behrend et. al., *A measurement of the π^0, η and η' electromagnetic form factors*, *Z.Phys.* **C49** (1991) 401–410.

[48] **CLEO** Collaboration, J. Gronberg et. al., *Measurements of the meson-photon transition form factors of light pseudoscalar mesons at large momentum transfer*, *Phys.Rev.* **D57** (1998) 33–54, [`hep-ex/9707031`].

[49] **BABAR** Collaboration, B. Aubert et. al., *Measurement of the $\gamma\gamma^* \to \pi^0$ transition form factor*, *Phys.Rev.* **D80** (2009) 052002, [`arXiv:0905.4778`].

[50] G. Amelino-Camelia, F. Archilli, D. Babusci, D. Badoni, G. Bencivenni et. al., *Physics with the KLOE-2 experiment at the upgraded DAϕNE*, *Eur.Phys.J.* **C68** (2010) 619–681, [`arXiv:1003.3868`].